J. Biochem. 2011;150(3):295–302 doi:10.1093/jb/mvr057

JB THE JOURNAL OF BIOCHEMISTRY

Crystal structure of the tandem-type universal stress protein TTHA0350 from *Thermus thermophilus* HB8

Received March 17, 2011; accepted April 9, 2011; published online May 18, 2011

Hitoshi Iino[1,2], Nobutaka Shimizu[3], Masaru Goto[1,4], Akio Ebihara[1], Kenji Fukui[1], Ken Hirotsu[1] and Seiki Kuramitsu[1,2,*]

[1]RIKEN SPring-8 Center, Harima Institute, 1-1-1 Kouto, Sayo, Hyogo 679-5148; [2]Department of Biological Sciences, Graduate School of Science, Osaka University, Toyonaka, Osaka 560-0043; [3]Research and Utilization Division, Japan Synchrotron Radiation Research Institute, 1-1-1 Kouto, Sayo, Hyogo 679-5198; and [4]Department of Biomolecular Science, Faculty of Science, Toho University, Funabashi, Chiba 274-8510, Japan

*Seiki Kuramitsu, RIKEN SPring-8 Center, Harima Institute, 1-1-1 Kouto, Sayo, Hyogo 679-5148, Japan. Tel: +81-791-58-2891, Fax: +81-791-58-2892, email: kuramitu@spring8.or.jp

The genome sequence of an extremely thermophilic bacterium, *Thermus thermophilus* HB8, revealed that TTHA0350 is a tandem-type universal stress protein (Usp) consisting of two Usp domains. Usp proteins, which are characterized by a conserved domain consisting of 130–160 amino acids, are inducibly expressed under a large number of stress conditions. The N-terminal domain of TTHA0350 contains a motif similar to the consensus ATP-binding one (G-2x-G-9x-G-(S/T)), but the C-terminal one seems to lack the consensus motif. In order to determine its structural properties, we determined the crystal structures of TTHA0350 in the unliganded form and TTHA0350•2ATP at 2.50 and 1.70 Å resolution, respectively. This is the first structure determination of a Usp family protein in both unliganded and ATP-liganded forms. TTHA0350 is folded into a fan-shaped structure which is similar to that of tandem-type Usp protein Rv2623 from *Mycobacterium tuberculosis*. However, the dimer assembly with C2-symmetry in TTHA0350 is quite different from that with D2-symmetry in Rv2623. The X-ray structure showed that not only the N-terminal but also the C-terminal domain binds one ATP, although the ATP-binding motif could not be detected in the C-terminal domain. The loop interacting with ATP in the C-terminal domain is in a conformation quite different from that in the N-terminal domain.

Keywords: pfam00582/structural genomics/thermophile/TTHA0350/universal stress protein.

Abbreviations: Usp, universal stress protein.

The universal stress protein (Usp) superfamily [Pfam accession number PF00582 (*1*)] is characterized by a conserved Usp domain consisting of 130–160 amino acids (*2–5*). More than 1000 Usp proteins are present in various organisms including bacteria, archaea and eukarya. Most Usp proteins occur as a single domain or two domains fused in tandem together. The expression of Usp proteins is induced under a large number of stress conditions; nutrient starvation and heat shock and with oxidants, uncouplers and DNA-damaging agents. However, the biochemical and molecular mechanism by which Usp proteins protect cells from stress remains unknown. ATP-binding Usp protein has been proposed to be a member of ancient HUP class, which was named after HIGH superfamily protein (Class I aminoacyl-t-RNA synthetase and various nucleotidyltransferase), Usp-like superfamily (Usp protein, photolyase and electron transferring flavoprotein) and PP(pyrophosphate)-loop ATPase (*6*). All HUP class domains have a common α/β structure as a core which is characterized by five-stranded parallel β-sheet with 3-2-1-4-5 order and four α-helices.

Three-dimensional structures of these Usp proteins give valuable clues for the understanding of their functions, although the biochemical roles of these proteins are not known. The X-ray structures of Usp proteins so far determined show that the Usp domain has a typical α/β structure common to HUP class domains (*2*). Some Usp proteins contain an ATP-binding consensus loop (G-2x-G-9x-G-(S/T)), others being free from this motif and lacking the ability to bind ATP (*3*). MJ0577, a single-domain Usp protein, from *Methanococcus jannaschii* is folded into a homodimer with 10-stranded β-sheet and binds one ATP per subunit (*7*). Preliminary biochemical experiments indicated that the protein is likely to act as an ATPase or an ATP-binding molecular switch like a G protein. Single-domain Usp protein HI0815 from *Haemophilus influenzae* also has a dimeric structure, which is similar to that of MJ0577 (*8*). However, ATP was not observed in the structure although the protein was crystallized in the presence of ATP, suggesting that the biochemical role of HI0815 is different. Recently, Rv2623, a tandem-type Usp protein, from *Mycobacterium tuberculosis* was shown to be involved in the ATP-dependent regulation of tuberculosis latency and to have a structure similar to those of the single-domain Usp proteins in a dimeric form (*9*).

The genome sequence of an extremely thermophilic bacterium, *Thermus thermophilus* HB8, published by the Structural-Biological Whole-Cell Project (www.thermus.org) (NCBI accession numbers NC_006461, NC_006462 and NC_006463), revealed that six Usp proteins belong to the Usp superfamily (Fig. 1). Three are single-domain ones, two tandem-type ones and one a component of probable potassium uptake

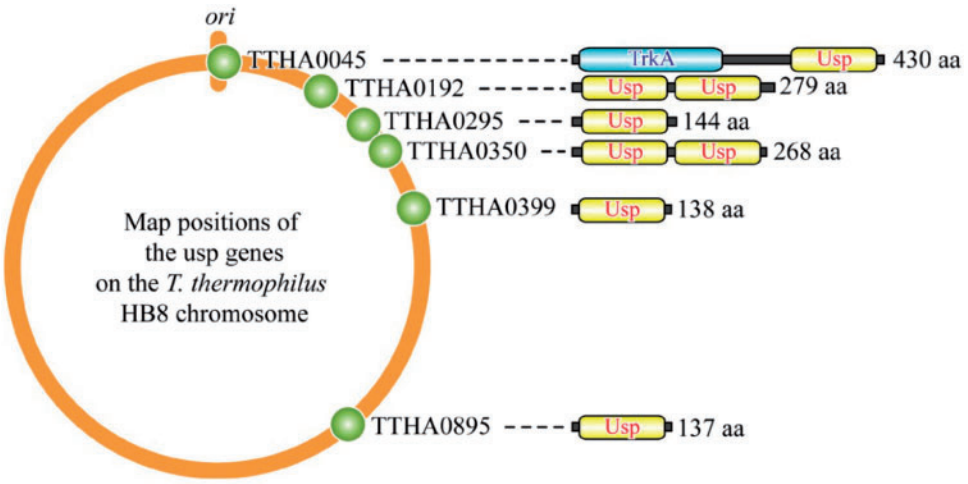

Fig. 1 Usp proteins of *T. thermophilus* HB8.

protein TrkA. Structure analysis of Usp proteins from *T. thermophilus* HB8, when their structures are combined with other related Usp protein structures so far determined, may contribute to the understanding of the ancient and conserved Usp superfamily and is thus important to the biochemical sciences. TTHA0350 is a tandem-type Usp protein consisting of two Usp domains. The N-terminal Usp domain contains a motif (G-2x-G-10x-G-S) similar to the consensus ATP-binding one, but the C-terminal one seems to lack the consensus motif because the corresponding sequence is G-8x-G-S (Fig. 2A). In order to determine its structural properties, we determined the crystal structures of TTHA0350 in the unliganded form and TTHA0350•2ATP at 2.50 and 1.70 Å resolution, respectively. This is the first structure determination of a Usp family protein in both unliganded and ATP-liganded forms.

Materials and Methods

Cloning, expression and purification

The *TTHA0350* gene was inserted between NdeI and the BamHI restriction site of plasmid pET-11 a (Novagen). The resulting expression plasmid was transformed into *Escherichia coli* strain BL21(DE3) (Novagen). The transformant was cultured at 310 K in 6 l of Luria broth supplemented with Ampicillin (100 μg ml^{-1}) (*10*). Cells were harvested by centrifugation after 16 h and stored at 193 K until use. In the native sequence, there is only one Met at position 1. Selenomethionine (SeMet)-substituted L171M was thus over-expressed in *E. coli* B834(DE3) cells grown in the presence of selenomethionine for single-wavelength anomalous dispersion (SAD) data collection. The replacement of Leu by Met at position 171 was considered to cause no change in the overall molecular structure. The protein was purified by incubation at 343 K for 10 min, ammonium sulphate fractionation and a three-step column chromatography procedure, first on a Resource Q column (GE Healthcare) equilibrated with 20 mM Tris–HCl, pH 8.0, followed by Resource ISO one (GE Healthcare) equilibrated with 50 mM sodium phosphate, pH 7.0, 0.75 M ammonium sulphate and finally on a HiLoad 16/60 Superdex 75 pg one (GE Healthcare) equilibrated with 20 mM Tris–HCl, pH 8.0, 150 mM NaCl.

Crystallization and data collection

Crystallization was performed at 293 K by using the sitting-drop or hanging-drop vapour diffusion method. SeMet-L171M crystals were obtained by equilibration of a mixture comprising of 1 μl protein solution (10.0 mg ml^{-1} protein, 20 mM Tris–HCl, pH 8.0) and 1 μl reservoir solution [100 mM sodium citrate, 9% (v/v) 2-methyl-2,4-pentanediol, 100 mM HEPES–NaOH, pH 7.8] against 100 μl of reservoir solution. Crystals of the unliganded form were obtained using 1 μl protein solution and 1 μl reservoir solution (500 mM magnesium formate, 100 mM HEPES–NaOH, pH 7.5) against 500 μl of reservoir solution. SeMet-L171M and unliganded crystals are isomorphous with a space group $P6_5$. Crystals of TTHA0350•2ATP grew in the presence of ATP on equilibration of a mixture comprising of 1 μl protein solution and 1 μl reservoir solution [8.6 mM ATP, 30 mM magnesium chloride, 40% (v/v) 1,2-propanediol, 100 mM sodium acetate trihydrate, pH 4.5] against 100 μl reservoir solution. A SAD data set for a SeMet-L171M crystal was collected to 2.62 Å resolution at 100 K using a wavelength of 0.97914 Å on the BL41XU station at SPring-8 (Hyogo, Japan). Data collection for the unliganded TTHA0350 and TTHA0350•2ATP crystals was performed at 100 K using a wavelength of 1.00000 Å on the BL26B2 station at SPring-8. The data were processed using HKL2000 (*11*).

Structure determination and refinement

The positions of all the four Se sites in the asymmetric unit were determined using the SAD data set for a SeMet-L171M with program SOLVE (*12*) and the resulting map was improved by solvent flattening with program RESOLVE (*13*). Nearly the entire backbone and most of the side chains could be traced with RESOLVE and ARP/wARP (*14*), respectively. Using the resultant structure of SeMet-L171M as the search model for the molecular replacement calculation, the initial structures for unliganded TTHA0350 and TTHA0350•2ATP were determined with AmoRe (*15*). The models were refined using programs CNS (*16*) and XtalView/Xfit (*17*) (Table I). The coordinates are available in the Protein Data Bank, under accession codes 3AB7 and 3AB8. Graphic figures were created using PyMOL (*18*), MOLSCRIPT (*19*) and RASTER3D (*20*).

Gel filtration chromatography

Size-exclusion chromatography was performed at 298 K on a HiLoad 16/60 Superdex 75 pg (GE Healthcare) using an ÄKTA system (GE Healthcare). A quantity of 3 ml aliquot of TTHA0350 (4 mg/ml) was loaded onto the column and eluted at the flow rate of 0.5 ml/min in 20 mM Tris–HCl, pH 8.0, 150 mM NaCl. The eluted proteins were detected by measuring the absorbance at 280 nm.

Dynamic light scattering

TTHA0350 (2.0 mg/ml) was prepared in 20 mM Tris–HCl, pH 8.0, 150 mM NaCl and transferred to a 0.02 μm, VectaSpin Micro centrifuge filter (Whatman). The 25 μl of the protein solution was loaded into a quartz cuvette and then analysed by Dynamic light scattering (DLS) instrument, DynaPro MSXTC/12/F with a gallium-arsenite diode laser, DynaPro-99-E-50 (Protein Solutions Inc.) at 298 K. The data were analysed using the Dynamics version 5.26.60 (Protein Solutions Inc.). The hydrodynamic radius value was

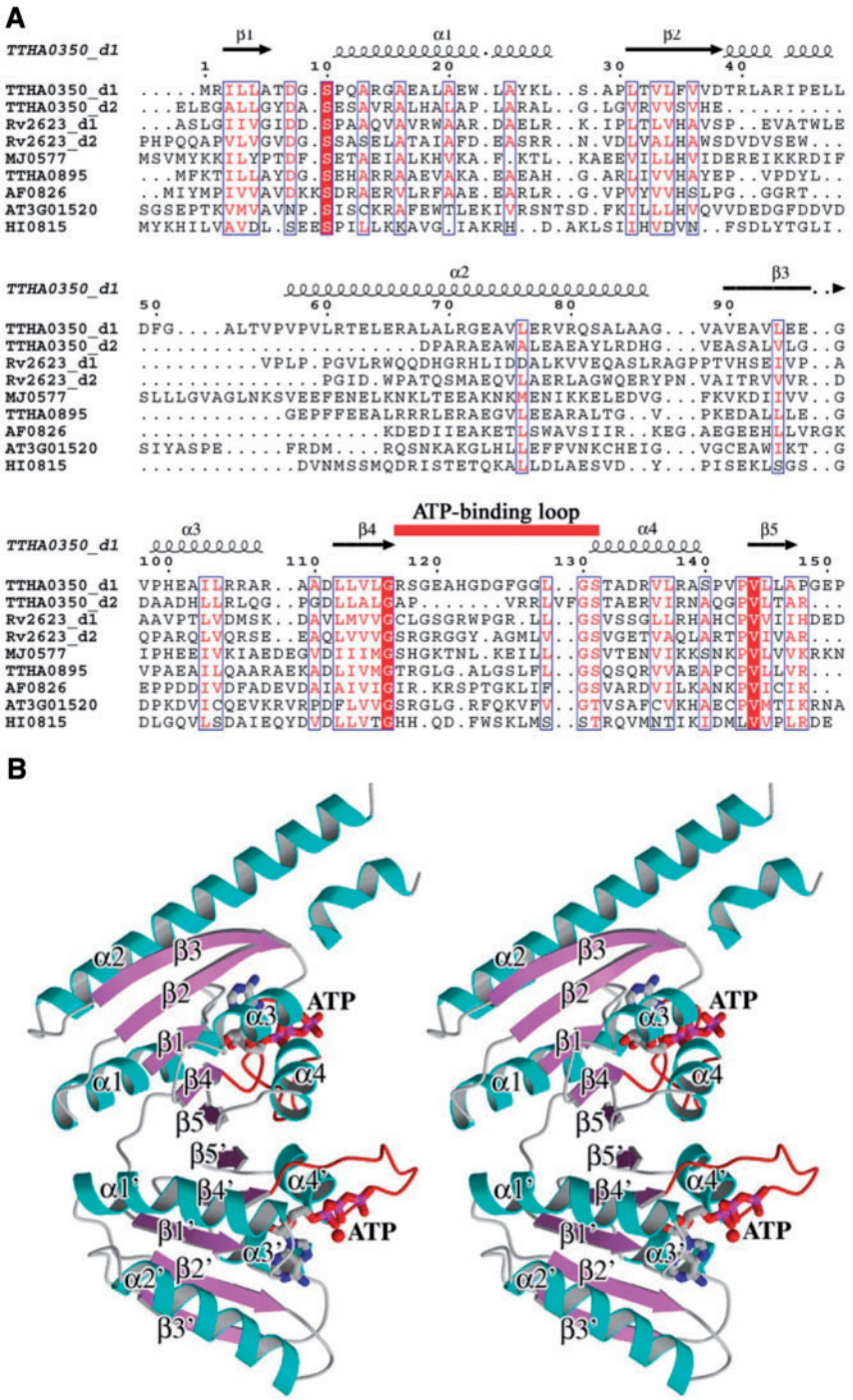

Fig. 2 Sequence alignment of Usp domains and crystal structure of TTHA0350 in ATP liganded form. (A) Structure-based sequence alignment and comparison of ATP-binding motif. Here, d1 and d2 are domains 1 and 2 of tandem-type Usp proteins. Strictly conserved and similar residues are boxed in red and represented by red letters, respectively. The figures were generated with ESPript 2.2 (*33*). (B) Stereoview of monomeric TTHA0350•2ATP viewed from the direction perpendicular to the pseudo 2-fold axis. ATP bound to the groove formed on the C-terminal side of the β-sheet is shown as a stick model (red). ATP-binding loops are shown in red.

calculated with the Stokes–Einstein equation using the obtained translational diffusion coefficient (*21*).

Isothermal titration calorimetry

Calorimetric data for the dilution of TTHA0350 solutions were obtained at 298 K using a VP-ITC MicroCalorimeter (Microcal) (*22*, *23*). The dilution experiment involved sequential injection of TTHA0350 solution (3.4 mg ml^{-1} protein, 20 mM Tris–HCl, pH8.0, 150 mM NaCl) into the calorimeter cell (1.4 ml) initially containing buffer alone, with an injection sequence of 30×10 µl at 4 min interval. A series of endothermic heat pulses were corrected for the heat of mixing of the components. Standard nonlinear least-squares method was used to fit experimental dilution data and obtain estimates of the dimerization binding constant ($K_{dim} = [P_2]/[P]^2$; $[P_2]$ and $[P]$ are the equilibrium concentrations of dimers and monomers, respectively) and the enthalpy of dimerization (ΔH_{dim}) assuming that the protein exists as a monomer or a dimer (*24*).

ATPase activity assay

Hydrolysis of ATP was measured at 25°C by an enzyme-coupled spectrophotometric assay (*25*). The change of absorbance at

Table I. Data collection and refinement statistics.

	Unliganded form	ATP complex
Diffraction data		
Space group	$P6_5$	$P1$
Cell dimensions		
a, *b*, *c* (Å)	126.9, 126.9, 76.9	38.9, 53.8, 63.4
α, β, γ (°)	90, 90, 120	78.9, 72.1, 69.7
Wavelength (Å)	1.00000	1.00000
Total number of reflections	258,615	134,896
No. of unique reflections	24,506 (2,435)[a]	47,774 (4,741)[a]
Completeness (%)	99.8 (100)[a]	95.5 (94.9)[a]
$I/\sigma(I)$	24.0 (5.9)[a]	27.7 (6.2)[a]
R_{merge} (%)[b]	4.8 (33.8)[a]	4.1 (13.7)[a]
Refinement		
Resolution limit (Å)	29.3–2.50	36.8–1.70
R_{factor} (%)	22.9	18.4
R_{free} (%)	27.3	21.8
No. of solvent atoms	58	460
Deviations		
Bond length (Å)	0.006	0.005
Bond angles (°)	1.3	1.3
Mean B factor		
Main chain atoms (Å^2)	58.8	12.8
Side chain atoms (Å^2)	59.6	17.7
Hetero atoms (Å^2)		11.1
Water molecules (Å^2)	52.1	26.0
Ramachandran plot (%)[c]	97.2; 2.8; 0.0; 0.0	96.7; 3.3; 0.0; 0.0

[a]The values in parentheses are for highest resolution shells (2.59–2.50 Å) in the unliganded form and (1.76–1.70 Å) in the ATP complex.
[b]$R_{merge} = \sum_{hkl} \sum_i |I_{hkl,i} - \langle I_{hkl} \rangle| \; / \; \sum_{hkl} \sum_i I_{hkl,i}$, where I = observed intensity and $\langle I \rangle$ = average intensity for multiple measurements.
[c]Percentages of residues in the most favoured, additionally allowed, generously allowed and disallowed regions of a Ramachandran plot (*34*).

340 nm was measured with a Hitachi spectrophotometer, model U-3010. ATP was reacted with 3 or 12 μM TTHA0350 in 50 mM Tris–HCl (pH 7.5), 100 mM KCl, 10 mM $MgCl_2$, 1 mM dithiothreitol, 2 mM phosphoenolpyruvate, 0.3 mM NADH, 5 μM pyruvate kinase and 5 μM lactate dehydrogenase at 25°C.

Results and Discussion

Overall Structure

The overall structure of tandem-type TTHA0350•2ATP is shown with secondary structure assignments made with program DSSP (*26*) in Fig. 2B. TTHA0350 consists of 268 amino acids residues with a molecular mass of 28,016 Da and is folded into a fan-shaped structure. The molecule is divided into two Usp domains, domains 1 (1–152) and 2 (153–268), the primary structure of domain 1 being 32% identical with that of domain 2. The domains share a common α/β-fold comprising of a five-stranded parallel β-sheet flanked by two α-helices from both sides of the sheet [SCOP 52436 (*27*)] although a long insert is present between β2 and α2 in domain 1 and the ATP-binding loop of domain 2 is five residues shorter than that of domain 1. The main chain of β-strand 5 in domain 1 is hydrogen bonded to the corresponding one (β-strand 5′) in domain 2 to form a 10-stranded β-sheet, the centre of which is penetrated by a pseudo 2-fold axis. The domain interface is characterized by hydrophobic stretches (P143-V144-L145-L146-A147 and P263-V264-L265-T266-A267) in β-strands 5 and 5′, respectively, which are well conserved in other related Usp proteins (Fig. 2A). Not only in β-strand 5 or 5′ but also in β-strands 1–4 or 1′–4′, hydrophobic clusters are involved in the formation of the stable β-sheet as a molecular core. The overall structure of TTHA0350 is similar to that of the dimer unit of the single-domain Usp from *M. jannaschii* (*7*) and that of the tandem-type Usp from *M. tuberculosis* (*9*).

The two subunits of TTHA0350 in the asymmetric unit form a dimer with a non-crystallographic 2-fold axis that is nearly parallel to the pseudo 2-fold axis of the monomer units (Fig. 3A). A surface area equivalent to 7.6% (877 Å^2) of one subunit is buried upon dimerization. The Cα atoms superimposition between the dimer units in the unliganded form (space group $P6_5$) and the ATP complex ($P1$) indicates that the dimer units in different crystallographic environments have the same structure except that the ATP-binding loops and the loops between β-strand 2 and α-helix 2 are disordered in the unliganded form. The molecular mass was estimated to be about 73 and 79 kDa roughly corresponding to that of the dimer by gel filtration and DLS experiment (hydrodynamic radius of 3.86 nm), respectively (Fig. 4A and B). The K_{dim} and the ΔH_{dim} have been calculated to be 2.24×10^5 M^{-1} and -384 kJ mol^{-1} at 298 K using the isothermal titration calorimetric data for the dilution of protein solutions (Fig. 4C). When the protein (subunit) concentration is equal to $1/K_{dim}$ (4.46×10^{-6} M), 50% of the protein is in the monomeric (or dimeric) form. At the first injection of the protein solution into the calorimetric cell, the protein concentration in the cell is estimated to be 8.67×10^{-7} M resulting in the monomer fraction of 77%. Combined, these results suggest that TTHA0350 exists as a homodimer as shown in Fig. 3A. Then, the structures of dimer models different from that shown in Fig. 3A were investigated (Supplementary Figs. S1–S4).

The hydrophobic effect of the dimerization is approximately estimated to be -21 to -27 kJ M^{-1} using the non-polar region (252 Å^2) of the subunit interface (*28*, *29*). This value is comparable with the unitary free energy change of the dimerization (-40.4 kJ M^{-1}) derived from K_{dim}. The overall fold of the monomer in TTHA0350 is similar to that of tandem-type Usp protein Rv2623. However, the dimer assembly with $C2$-symmetry in TTHA0350 is quite different from that with $D2$-symmetry in Rv2623 (Fig. 3A and B). In TTHA0350, the dimeric structure is characterized by 16 salt bridges between Arg and Glu or Asp, which occur on one side of the fan-like monomer unit (*30*). In Rv2623, the dimer interface predominantly consists of hydrophobic residues such as Trp, Val, Leu and Tyr, which are located around the edge of the fan.

ATP-binding in TTHA0350

Upon approach of ATP molecules, the ATP-binding loop of domains 1, which is disordered in the unliganded form, show its ordered structure to interact with the triphosphate moiety of ATP (Figs. 3A and 5). ATP-binding loop of domain 2 changes its

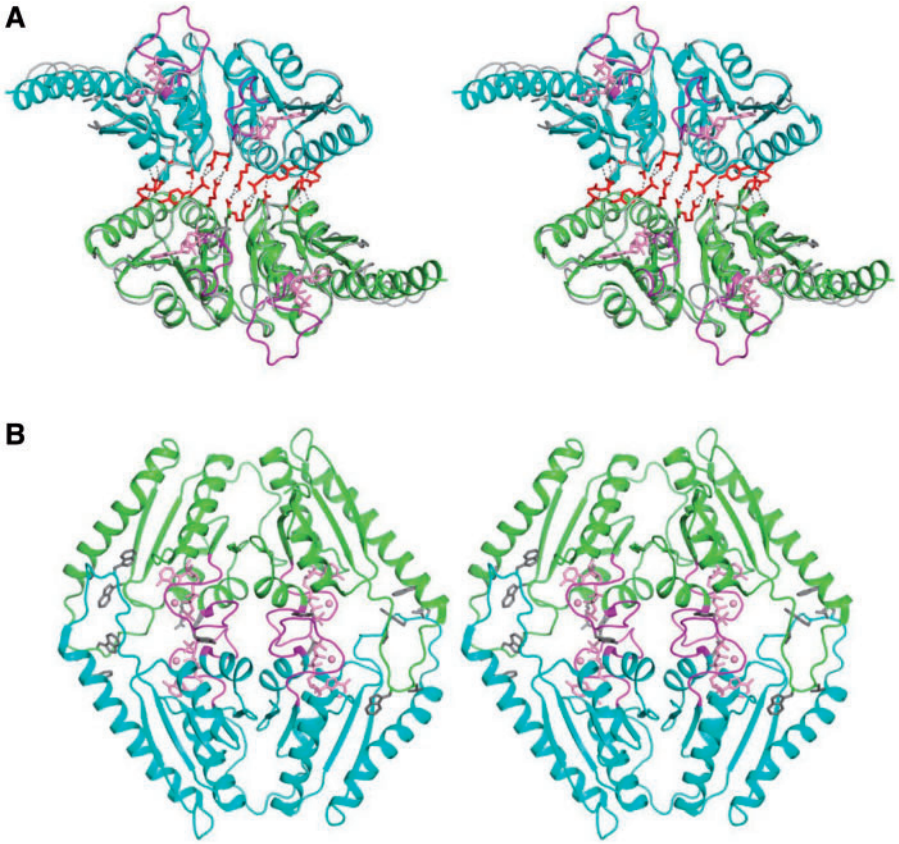

Fig. 3 Stereoview of the overall structures. (A) Dimeric TTHA0350 viewed down the molecular 2-fold axis. The complex with ATP is superimposed on the unliganded form by means of least-squares fitting of Cα atoms. The unliganded form is represented by line ribbons (grey). One subunit of the complex is drawn in blue and the other in green. Arg, Glu and Asp residues involved in salt bridges (dotted lines) between two subunits are represented by stick models (red). ATP is shown as a stick model (pink). The ATP-binding loop is shown in magenta. (B) Dimeric Rv2623 viewed down the molecular 2-fold axis. Hydrophobic residues concerned with dimer formation are shown in stick models (grey). ATP and the ATP-binding loop are shown in pink and magenta, respectively.

conformation and binds the triphosphate moiety of ATP in a loop structure quite different from that of domain 1. The average temperature factors for the loops of domains 1 and 2 in TTHA0350•2ATP are 14.7 and 11.3 $Å^2$, which are comparable with those of main or side chain atoms (Table II). Spectroscopic measurement of ATPase activity by a coupled assay indicated that TTHA0350 has no activity (Fig. 4D). The ATP-binding Usp domains, the structures of which have so far been determined, have a similar conformation of ATP-binding loops with a consensus motif, G-2x-G-9x-G-(S/T) (*7*, *9*) (Fig. 2A, shown as a red belt). The arrangements and conformations of bound ATP molecules are also conserved in these Usp proteins.

Domain 1 of TTHA0350 was found to contain an ATP-binding loop (G-2x-G-10x-G-S), which is similar to, but one residue longer than the consensus one, is folded into a conformation similar to that of the conserved one with the conserved arrangement of the bound ATP. However, in the case of domain 2, the ATP-binding motif could not be detected on sequence alignment. The X-ray structure showed that not only domain 1 but also domain 2 binds one ATP, although the loop interacting with ATP in domain 2 is in a conformation quite different from that in domain 1 (Fig. 5). The sequence alignment based on the three-dimensional structures of TTHA0350 and other related Usp proteins showed that the motif in domain 2 is G-8x-G-S (Fig. 2A). This is unusual in that the motif is lacking the second conserved Gly, is four residues short, and is folded into a conformation different from that of the conserved one. The arrangement of the terminal pyrophosphate moiety of ATP pyrophosphate is also significantly different from the conserved one (Fig. 5). The accessible surface area (ASA) of the bound ATP in domain 2 is 76.5 $Å^2$, which is significantly larger than the corresponding value (46.9 $Å^2$) in domain 1. These results suggest that not only the binding affinity of ATP but also the role of the ATP-binding loop is different between domains 1 and 2. At the present stage, it is not known whether the motif, G-8x-G-S, is a new ATP-binding one or a variety of loops interacts with the ATP pyrophosphate. The adenosine binding cavities in Usp protein structures so far determined have a similar shape irrespective of the unliganded form or ATP liganded one. The interactions of the adenosine moiety of ATP with the cavity in TTHA0350 are common to domains 1 and 2 and are mostly conserved in other related ATP-binding Usp domains.

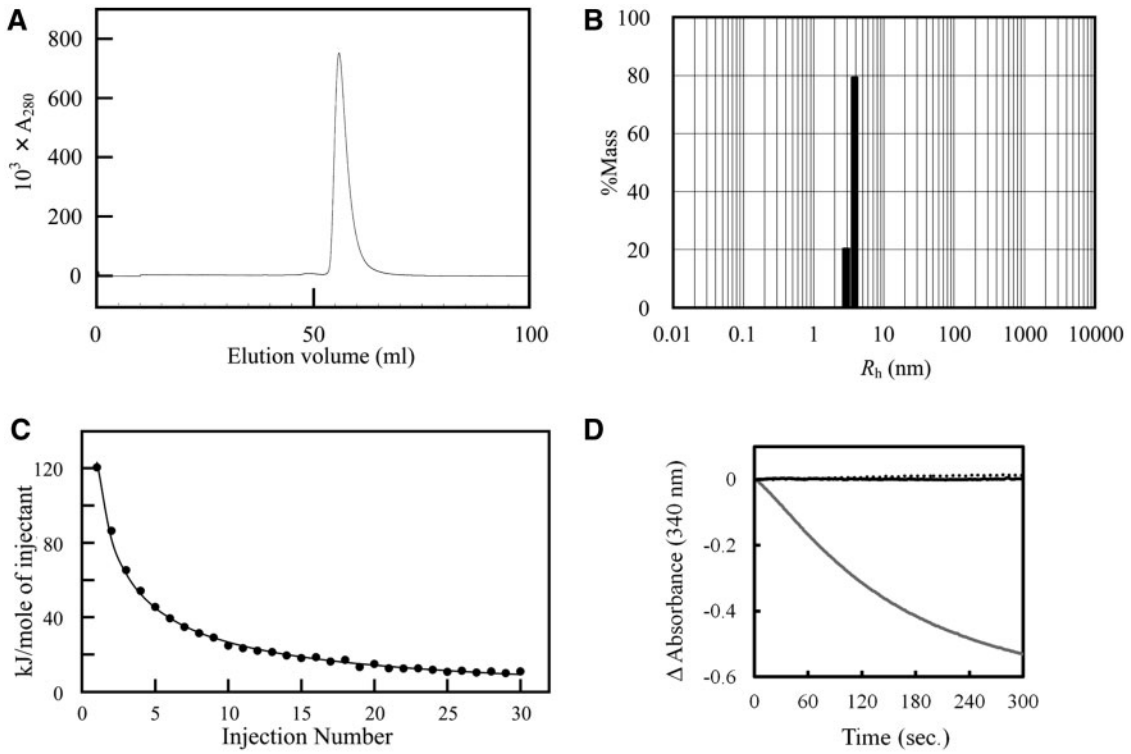

Fig. 4 Biochemical properties of TTHA0350. (A) Gel filtration chromatography (B) Dynamic light scattering. R_h is the hydrodynamic radius. The '%Mass' represents the estimated relative amount of mass (concentration) of each species. (C) Isothermal titration calorimetry. The solid line represents the best fit of the data by standard nonlinear least-squares method. (D) Spectroscopic measurement of ATPase activity. Measurements were made in the pyruvate kinase–lactate dehydrogenase-coupled assay in the presence of 10 mM ATP and 3 μM (solid line) or 12 μM (dotted line) TTHA0350. A control (grey line) with 10 mM ADP instead of ATP in the absence of TTHA0350 was carried out to verify the decay of 340 nm absorbance.

Table II. Structural similarity between TTHA0350 and other related Usp domains.

Species	Molecule	Z[a]		% id[b]		Pdb code	ATP-binding consensus motif
		d1[c]	d2[c]	d1	d2		
Methanococcus jannaschii	MJ0577	20.0	14.0	27	21	1mjh	G-2x-G-9x-G-S
Mycobacterium tuberculosis	Rv2623-d1[d]	18.8	14.3	24	17	3cis	G-2x-G-9x-G-S
Thermus thermophilus HB8	TTHA0895	18.0	16.0	44	35	2z09	G-2x-G-9x-G-S
Mycobacterium tuberculosis	Rv2623-d2[d]	17.1	–	23	–	3cis	G-2x-G-9x-G-S
Archeoglobus fulgidus	AF0826	17.1	16.0	20	27	3dlo	G -12x-G-S
Arabidopsis thaliana	AT3G01520	–	15.0	–	18	2gm3	G-2x-G-9x-G-S
Haemophilus influenzae	HI0815[e]	12.2	10.7	20	19	1jmv	–

[a]DALI *Z* score (strength of structural similarity).
[b]Primary structure identity.
[c]d1 and d2 are domains 1 and 2 of TTHA0350, respectively.
[d]Rv2623-d1 and Rv2623-d2 are domains 1 and 2 of Rv2623, respectively.
[e]HI0815 lacks ATP-binding activity and the consensus motif.

Structural comparison of TTHA0350 with ATP-binding Usp proteins

Program Dali (*31*, *32*) was used to search the Protein Data Bank database for proteins possessing three-dimensional structures similar to that of domain 1 or 2 of TTHA0350. The five exhibiting the highest *Z*-scores (strength of structural similarity) were selected and are listed in Table II, including the Usp protein from *H. influenzae*, which lacks ATP-binding ability. Out of the first five structures similar to that of domain 1 or 2 of TTHA0350, four (MJ0577, domain 1 of Rv2623, TTHA0895 and AF0826) are common to both domains. The *Z*-values range from 17.1 to 20.0 and from 14.0 to 16.0 for domains 1 and 2, respectively. This indicates that the overall structures of these Usp proteins (domains) are very similar to each other. The primary structure identities are in the range of 20–44% and 18–35% for domains 1 and 2, respectively, and there seems to be no strong correlation between the strength of structural similarity and sequence identity (Table II). The consensus ATP-binding motif, G-2x-G-9x-G-S, is present in five Usp domains (domains 1 and 2 of Rv2623, MJ0577, TTHA0895 and AT3G01520) in Table II, which have

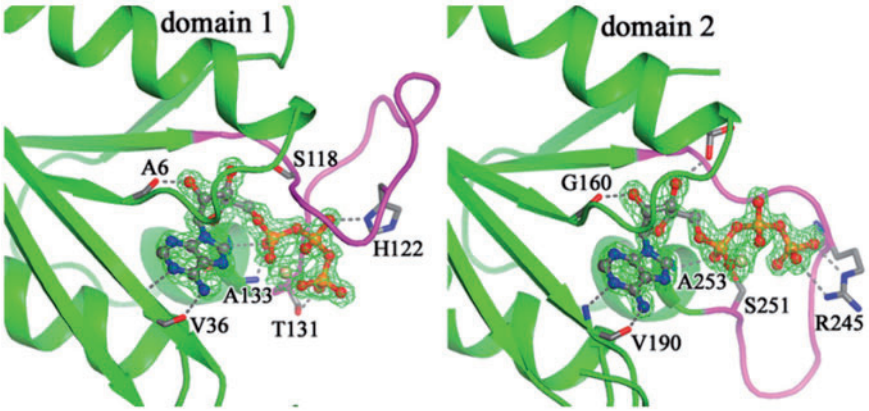

Fig. 5 ATP binding in domain 1 and 2. ATP, main chain NH and C=O groups and side-chains interacting with ATP are represented by stick models. The ATP-binding loop is shown in magenta. Hydrogen bond/salt bridge interactions are represented by dotted lines. The omit electron density map for the bound ATP is contoured at the 1.5 σ level. The ATP-binding loop in the unliganded form (wheat) is superposed.

been shown to bind ATP (AMP for AT3G01520) by X-ray analyses. The superposition of AT3G01520 on ATP-binding Usp proteins in Table II suggests that ATP as well as AMP is accommodated in a cavity similarly to these Usp proteins. In AF0826, a motif (G-12x-G-S), which is the same as the consensus one except for the lack of second conserved Gly residue, was recognized in the region corresponding to the ATP-binding loop in other related proteins. The superimposition of AF0826 in the unliganded form onto domain 1 of TTHA0350 or MJ0577 in the ATP liganded form indicates that the adenosine binding cavity quite similar to that in TTHA0350 or MJ0577 is formed at the N-terminal side of the β-sheet in AF0826. Presumably, the cavity of AF0826 may accommodate the adenosine moiety of ATP and its consensus loop may interact with the triphosphate of ATP by reorienting the loop conformation.

Supplementary Data

Supplementary Data are available at *JB* online.

Acknowledgements

The authors wish to thank Kayoko Matsumoto and Yumiko Inoue for protein expression and purification and Yoshiaki Kitamura for data collection at SPring-8. The synchrotron-radiation experiments were performed at BL26B2 and BL41XU in SPring-8 (Harima, Japan). The X-ray diffraction experiments at the SPring-8 beamline BL41XU were performed under the approval of the Japan Synchrotron Radiation Research Institute Program Advisory Committee (proposal 2006B1388).

Conflict of interest
None declared.

References

1. Bateman, A., Birney, E., Durbin, R., Eddy, S.R., Howe, K.L., and Sonnhammer, E.L. (2000) The Pfam protein families database. *Nucleic Acids Res.* **28**, 263–266
2. Kvint, K., Nachin, L., Diez, A., and Nystrom, T. (2003) The bacterial universal stress protein: function and regulation. *Curr. Opin. Microbiol.* **6**, 140–145
3. Siegele, D.A. (2005) Universal stress proteins in Escherichia coli. *J. Bacteriol.* **187**, 6253–6254
4. Weber, A. and Jung, K. (2006) Biochemical properties of UspG, a universal stress protein of Escherichia coli. *Biochemistry* **45**, 1620–1628
5. Nachin, L., Brive, L., Persson, K.C., Svensson, P., and Nystrom, T. (2008) Heterodimer formation within universal stress protein classes revealed by an in silico and experimental approach. *J. Mol. Biol.* **380**, 340–350
6. Aravind, L., Anantharaman, V., and Koonin, E.V. (2002) Monophyly of class I aminoacyl tRNA synthetase, USPA, ETFP, photolyase, and PP-ATPase nucleotide-binding domains: implications for protein evolution in the RNA. *Proteins* **48**, 1–14
7. Zarembinski, T.I., Hung, L.W., Mueller-Dieckmann, H.J., Kim, K.K., Yokota, H., Kim, R., and Kim, S.H. (1998) Structure-based assignment of the biochemical function of a hypothetical protein: a test case of structural genomics. *Proc. Natl Acad. Sci. USA* **95**, 15189–15193
8. Sousa, M.C. and McKay, D.B. (2001) Structure of the universal stress protein of Haemophilus influenzae. *Structure* **9**, 1135–1141
9. Drumm, J.E., Mi, K., Bilder, P., Sun, M., Lim, J., Bielefeldt-Ohmann, H., Basaraba, R., So, M., Zhu, G., Tufariello, J.M., Izzo, A.A., Orme, I.M., Almo, S.C., Leyh, T.S., and Chan, J. (2009) Mycobacterium tuberculosis universal stress protein Rv2623 regulates bacillary growth by ATP-Binding: requirement for establishing chronic persistent infection. *PLoS Pathog.* **5**, e1000460
10. Sambrook, J., Fritsch, E.F., and Maniatis, T. (1982) *Molecular Cloning: a Laboratory Manual*., Cold Spring Harbor Laboratory Press, New York
11. Otowinowski, Z. and Minor, W. (1997) Processing of X-ray diffraction data collected in oscillation mode. *Methods Enzymol.* **276**, 307–326
12. Terwilliger, T.C. and Berendzen, J. (1999) Automated MAD and MIR structure solution. *Acta Crystallogr.* **D55**, 849–861
13. Terwilliger, T.C. (2000) Maximum-likelihood density modification. *Acta Crystallogr.* **D56**, 965–972
14. Morris, R.J., Perrakis, A., and Lamzin, V.S. (2002) ARP/wARP's model-building algorithms. *I. The main chain. Acta Crystallogr.* **D58**, 968–975
15. Navaza, J. (1994) AMoRe: an automated package for molecular replacement. *Acta Crystallogr.* **A50**, 157–163

16. Brunger, A.T., Adams, P.D., Clore, G.M., DeLano, W.L., Gros, P., Grosse-Kunstleve, R.W., Jiang, J.S., Kuszewski, J., Nilges, M., Pannu, N.S., Read, R.J., Rice, L.M., Simonson, T., and Warren, G.L. (1998) Crystallography & NMR system: A new software suite for macromolecular structure determination. *Acta Crystallogr*. **D54**, 905–921
17. McRee, D.E. (1999) XtalView/Xfit–A versatile program for manipulating atomic coordinates and electron density. *J. Struct. Biol*. **125**, 156–165
18. DeLano, W. (2002) *The PyMOL User's Manual*. DeLano Scientific, San Carlos, CA
19. Kraulis, P.J. (1991) MOLSCRIPT: a program to produce both detailed and schematic plots of protein structures. *J. Appl. Crystallogr*. **24**, 946–950
20. Merritt, E.A. and Murphy, M.E. (1994) Raster3D Version 2.0. A program for photorealistic molecular graphics. *Acta Crystallogr*. **D50**, 869–873
21. Ruf, H., Georgalis, Y., and Grell, E. (1989) Dynamic laser light scattering to determine size distributions of vesicles. *Methods Enzymol*. **172**, 364–390
22. Wiseman, T., Williston, S., Brandts, J.F., and Lin, L.N. (1989) Rapid measurement of binding constants and heats of binding using a new titration calorimeter. *Anal. Biochem*. **179**, 131–137
23. Leavitt, S. and Freire, E. (2001) Direct measurement of protein binding energetics by isothermal titration calorimetry. *Curr. Opin. Struct. Biol*. **11**, 560–566
24. McPhail, D. and Cooper, A. (1997) Thermodynamics and kinetics of dissociation of ligand-induced dimers of vancomycin antibiotics. *J. Chem. Soc., Faraday Trans*. **93**, 2283–2289
25. Guthapfel, R., Gueguen, P., and Quemeneur, E. (1996) ATP binding and hydrolysis by the multifunctional protein disulfide isomerase. *J. Biol. Chem*. **271**, 2663–2666
26. Kabsch, W. and Sander, C. (1983) Dictionary of protein secondary structure: pattern recognition of hydrogen-bonded and geometrical features. *Biopolymers* **22**, 2577–2637
27. Murzin, A.G., Brenner, S.E., Hubbard, T., and Chothia, C. (1995) SCOP: a structural classification of proteins database for the investigation of sequences and structures. *J. Mol. Biol*. **247**, 536–540
28. Fersht, A. (1998) *Structure and Mechanism in Protein Science: A Guide to Enzyme Catalysis and Protein Folding*. W. H. Freeman, New York
29. CCP4. (1994) The CCP4 suite: programs for protein crystallography. *Acta Crystallogr*. **D50**, 760–763
30. Reynolds, C., Damerell, D., and Jones, S. (2009) ProtorP: a protein-protein interaction analysis server. *Bioinformatics* **25**, 413–414
31. Holm, L. and Park, J. (2000) DaliLite workbench for protein structure comparison. *Bioinformatics* **16**, 566–567
32. Holm, L. and Sander, C. (1993) Protein structure comparison by alignment of distance matrices. *J. Mol. Biol*. **233**, 123–138
33. Gouet, P., Courcelle, E., Stuart, D.I., and Metoz, F. (1999) ESPript: analysis of multiple sequence alignments in PostScript. *Bioinformatics* **15**, 305–308
34. Laskowski, R.A., MacArthur, M.W., Moss, D.S., and Thornton, J.M. (1993) PROCHECK: a program to check the stereochemical quality of protein structures. *J. Appl. Crystallogr*. **26**, 283–291